Review of Scientific Instruments

RESEARCH ARTICLE | MAY 19 2023

Calibrating beam fluxes of a low-energy neutral atom beam facility

Jonathan Gasser ; André Galli ; Peter Wurz

Rev Sci Instrum 94, 053302 (2023)
https://doi.org/10.1063/5.0140759

AIP Publishing

Review of Scientific Instruments ARTICLE scitation.org/journal/rsi

Calibrating beam fluxes of a low-energy neutral atom beam facility

Cite as: Rev. Sci. Instrum. 94, 053302 (2023); doi: 10.1063/5.0140759
Submitted: 30 December 2022 • Accepted: 5 May 2023 •
Published Online: 19 May 2023

Jonathan Gasser,[a] André Galli, and Peter Wurz

AFFILIATIONS

University of Bern, Physics Institute, Space Research and Planetary Sciences, Sidlerstrasse 5, 3012 Bern, Switzerland

[a]Author to whom correspondence should be addressed: jonathan.gasser@unibe.ch

ABSTRACT

Scientific detection and imaging instruments for low-energetic neutral atoms (ENA) onboard spacecraft require thorough pre-flight laboratory calibration against a well-characterized neutral atom beam source. To achieve this requirement, a dedicated test facility is available at the University of Bern, which is equipped with a powerful plasma ion source and an ion beam neutralization stage. Using surface neutralization, low-energy neutral atom beams of any desired gas species can be produced in the energy range from 3 keV down as low as 10 eV. As the efficiency of the neutralization stage is species and energy dependent, the neutralizer itself needs to be calibrated against an independent reference. We report on the calibration and characterization of this neutral atom beam source using our recently developed Absolute Beam Monitor (ABM) as a primary calibration standard. The ABM measures the absolute ENA flux independent of neutral species in the energy range from 10 eV to 3 keV. We obtain calibration factors of a few 100 cm^{-2} s^{-1} pA^{-1}, depending on species at beam energies above about 100 eV, and a power-law decrease for energies below 100 eV. Furthermore, the energy loss of neutralized ions in the surface neutralizer is estimated from time-of-flight measurements using the ABM. The relative energy loss increases with ENA energy from low levels near zero up to 20%–35% at 3 keV, depending on atomic species. Having calibrated our neutral beam source allows for accurate calibration of ENA space instruments.

I. INTRODUCTION

Remote observation of plasma populations using energetic neutral atoms (ENA) onboard spacecraft is an established observation technique in space and planetary science.[1] This is owed to the production mechanism of an ENA in space: an energetic ion exchanges its charge with an ambient neutral atom. In interplanetary space, when particle–particle collisions are negligible, the resulting ENA is no longer affected by electric or magnetic fields so that the newly created ENA leaves its region of origin with the energy, velocity, and direction of the parent ion. ENA imaging thus allows us to study extended plasma regions in space, e.g., planetary magnetospheres or the heliosphere, from a remote vantage point.[2]

Specifically, the Interstellar Boundary Explorer (IBEX) mission by NASA[3] remotely explores interactions between the solar wind and the interstellar medium at the heliopause using two ENA imaging instruments, IBEX-Lo[4] and IBEX-Hi.[5] All-sky mapping of heliospheric ENA (mainly hydrogen and oxygen, but also helium and deuterium) at a wide range of energy bands has led to a much deeper understanding of the general physical properties of our heliosphere. For instance, it has led to the discovery of the unanticipated "IBEX ribbon"[6–8] of the heliosphere. After 15 years of successful operation of IBEX covering more than one full solar cycle, solar cycle effects in the heliosphere can be studied.[9] The successor Interstellar Mapping and Acceleration Probe (IMAP)[10] mission is scheduled for launch in early 2025. It will further extend our understanding of the heliosphere and its interaction with the interstellar medium. Three ENA instruments covering complementary energy ranges are included in IMAP's suite of ten scientific instruments, to analyze heliospheric ENA and interstellar neutral atoms (ISN). ENA imaging and analysis instruments have also been flown successfully on several other planetary missions (see Ref. 11 and references therein).

Scientific instruments for ENA detection and analysis must include an efficient ionization method, suitable for application in a space instrument, of the incident neutral atoms prior to their mass and energy analysis by ion-optical means.[1] ENA above an energy threshold of about 1 keV can be ionized by stripping off an electron in letting them pass through a micrometer-thin carbon foil.[12]

This ionization technique is applied, among others, in the IBEX-Hi instrument.[5]

At lower energies, particle transmission through the foil strongly decreases, so an alternative ionization method must be applied. To date, the widest applied ionization method for low-energy ENA that is also suitable for space applications is via grazing-incidence angle surface scattering.[1] Among the most efficient and widest applied charge-conversion surface (CS), materials in space instrumentation are aluminum oxide (Al_2O_3)[13] and diamond-like carbon (DLC) materials;[14,15] however, several other materials have been characterized experimentally and shown suitable as well (see Ref. 16 and references therein).

The applied ionization method, negative ionization via surface scattering, inherently introduces some angular spread of the ionized atoms as well as a reduction in their kinetic energy due to the surface interaction. Both effects depend on atomic species, incidence angle, and ENA energy. This may affect the overall instrument throughput and analysis. Like other instruments, low-energy ENA instruments rely on thorough laboratory calibration against a well-characterized neutral atom beam source. Substituting the ENA beam with an ion beam would greatly simplify the calibration preparations and procedure, as ion beams can be prepared and characterized much easier by standard means. However, this is not feasible for low-energy ENA instrument calibration, as low-energy ions are affected by electric fields inside the ENA instrument.

II. LABORATORY SETUP

An overview of the experimental setup is shown in Fig. 1 and is briefly described in the following. The entire experiment setup is described in more detail in Gasser *et al.* (2022).[11]

The MEFISTO calibration facility[17] at the University of Bern is used for laboratory calibrations of scientific ion and ENA imaging space flight instrumentation. Originally designed and built for solar wind experiments, the large MEFISTO vacuum test chamber is equipped with a powerful microwave-heated plasma ion source[18–20] and subsequent ion-optical system to produce a collimated beam of positive ions from any desired gas species and guide it into the main vacuum chamber (Fig. 1, left). The calibration campaign of the IBEX-Lo instrument was carried out in MEFISTO,[4] and the IMAP-Lo instrument will be calibrated here as well. The IMAP-Lo calibration campaign will include H, He, O, Ne, and D calibrated ENA beams in the energy range of 10 eV to 1 keV.

The necessary low-energy ENA beams are produced by converting a 3 keV ion beam using surface neutralization at grazing incidence angle. For this purpose, a surface neutralizer[21] is installed in front of the ion beam entrance into the vacuum chamber (Fig. 1, center). The ion beam enters the neutralizer and is decelerated by floating the neutralizer to an electrical potential of up to 3 kV. The energy E_{ion}/q of the ion beam striking the neutralizing tungsten single crystal surface is set by adjusting the float high voltage in combination with a 20° electrostatic analyzer (ESA) in the neutralizer,

$$\frac{E_{ion}}{q} = U_{extr} - U_{float} = k_{eff} \cdot U_{ESA}.$$

The effective neutralizer ESA constant is $k_{eff} \triangleq 10$, and $-U_{ESA}$ and $+U_{ESA}$ are the bias voltages applied to the inner and outer ESA electrodes, respectively.

After on-surface neutralization, remaining positive and converted negative ions are removed from the scattered beam by two electrostatic deflection plates. These plates are sawtooth baffled to enhance the absorption of ions out of the beam path and prevent neutralized atoms from being reflected towards the exit aperture. The neutral atom beam is collimated through a 16 × 16 mm^2 exit aperture, resulting in an angular beam spread of approximately ±5.5° in horizontal and ±4° in vertical extent. The surface neutralizer is mounted on a two-axis linear translation stage, which allows for precise positioning of the neutralizer entrance aperture with respect to the ion beam in the plane perpendicular to the ion beam axis. This is important because the ion beam location may vary with the plasma conditions in the ion source and the optimization of the ion beam path.

The beam neutralization process using a neutralizing surface causes a reduction of the beam energy and an increase in the neutral beam angular divergence. This implies that the produced ENA beam exiting the neutralizer needs to be characterized separately. Until recently, the neutral beam flux was determined using a standard particle detector such as an MCP detector. The accuracy of the neutral atom flux measurement is, however, limited by the knowledge of the detector's detection efficiency for neutral atoms at the energies of interest. To improve on this problem, we recently developed an

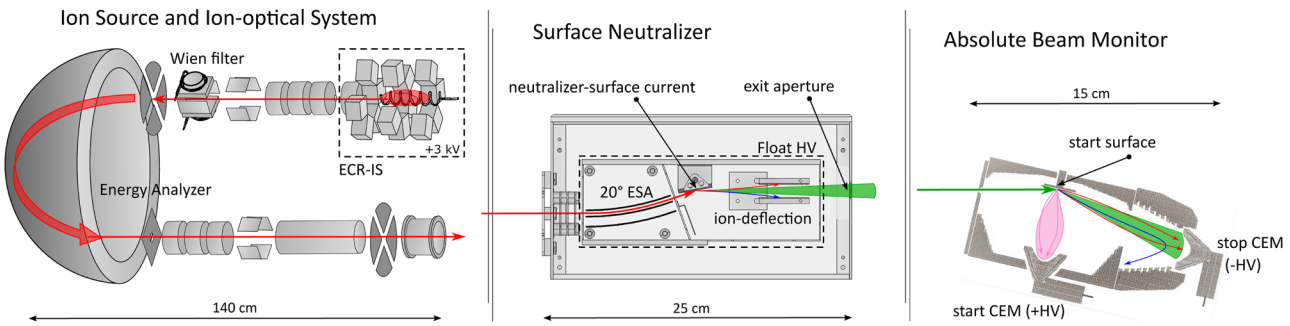

FIG. 1. Scheme of the experimental setup of the MEFISTO calibration facility: on the left, the plasma ion source and ion-optical system; in the center, the surface neutralizer; and to the right, the absolute beam monitor. Units are shown at different scales.

Absolute Beam Monitor (ABM),[11] which allows us to experimentally determine the absolute neutral atom flux F_n from the neutralizer without relying on prior knowledge of detector efficiencies.

Aside from the primary ion beam energy and species, the actual ENA beam intensity largely depends on the ion beam intensity from the ion source, which is strongly affected by the detailed plasma conditions in the ion source and is subject to optimization of the downstream ion-optical system. Consequently, the intensity of the ion beam into the neutralizer varies from day to day and may also vary during operating time. We keep track of these ion beam intensity variations by real-time monitoring the current recorded on the neutralizer surface used for beam-neutralizing using a pico-amperemeter installed in the neutralizer itself.

We verified that the neutral atoms flux into the chamber, for a given species and beam energy, is proportional to the neutralizer surface current. This is justified because in particle scattering surface interactions at grazing incidence angles, the fraction of neutralized ions and the angular scatter distribution vary with incident ion energy, species, and incidence angle but are not observed to deviate from proportionality with ion beam intensity. Since the neutralizer surface is a tungsten metal surface, even high ion intensities will not lead to surface charging. To calibrate the neutralizer, we relate the ENA flux F_n out of the neutralizer measured by the ABM to the neutralizing surface current I_{ncs} measured in the neutralizer itself. The surface current I_{ncs} then serves as a secondary reference during the ENA instrument calibrations and converts to the ENA flux by a calibration factor,

$$CF(E_{ion}) = F_n/I_{ncs},$$

as a function of the ion beam energy E_{ion} for a set of ion species of interest. For example, for a neutralizer surface current of I_{ncs} = 1 nA, the calibration factor CF = 1000 s^{-1} cm^{-2} pA^{-1} corresponds to a neutral atom beam flux of $F_n = 10^6$ s^{-1} cm^{-2} in the test chamber. With the ABM, we measure the absolute neutral atoms flux locally in the test chamber, as described in Ref. 11.

We calibrated the MEFISTO laboratory neutral beam source for a set of atomic species of particular interest in regard to the IMAP-Lo calibration campaign using the ABM as an independent primary calibration standard.

III. RESULTS AND DISCUSSION

A. Absolute neutral atom flux

In Figs. 2–6, the calibration factor CF as determined from the ABM flux and simultaneous neutralizer surface current measurements is plotted as a function of the primary ion beam energy for hydrogen, helium, deuterium, oxygen, and sulfur atom beams, respectively. The measured data were fitted with a three-parameter Weibull distribution function,[11]

$$f(x) = a\left(1 - \exp\left(-(x/b)^d\right)\right), \quad (1)$$

where a represents the asymptotic CF at high energies, b represents the roll-over energy (see below), and d represents the power-law exponent at low energies. This fit function was chosen because it represents the measured data well but without derivation or direct physical interpretation. Above characteristic roll-over energy of

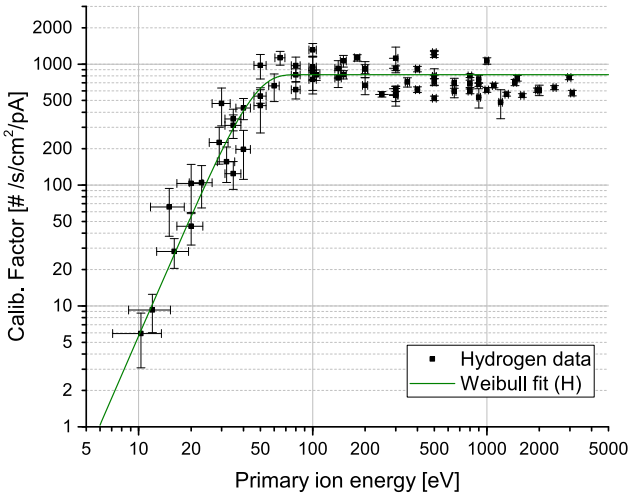

FIG. 2. Calibration factor ($CF = F_n/I_{ncs}$) for hydrogen in the ion energy range from 10 eV to 3 keV.

around 100 eV, the ENA flux out of the neutralizer does not depend on ion energy and is proportional to the neutralizer surface current. Below this roll-over energy, the measured data show a power-law relationship between the CF and primary ion energy, depending on the ENA species. The ion beam has a finite temperature, i.e., an angular divergence. Upon deceleration, this angular divergence grows, and when it exceeds, the acceptance of the energy analyzer in the neutralizer the transmission is reduced accordingly. This results in the power-law decline of the signal below the roll-over energy.

The primary contributions to the measurement uncertainty of the CF in the low-energy range are the low coincidence counting statistics from the ABM. The uncertainty in the energy results from the limited accuracy of the voltage difference between the neutralizer

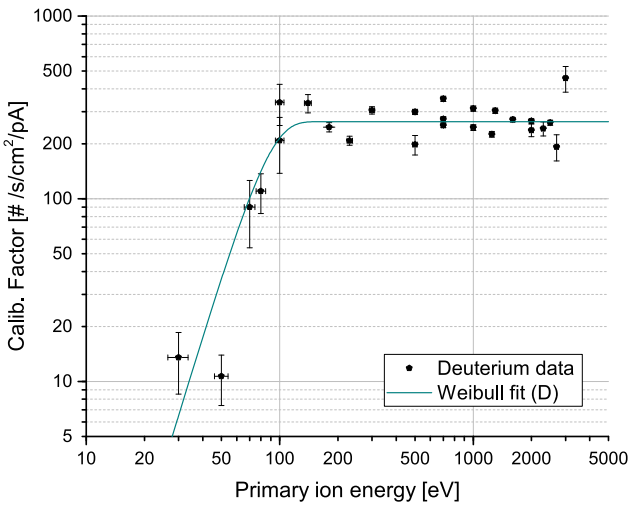

FIG. 3. Neutralizer calibration factor for deuterium in the energy range from 30 eV to 3 keV.

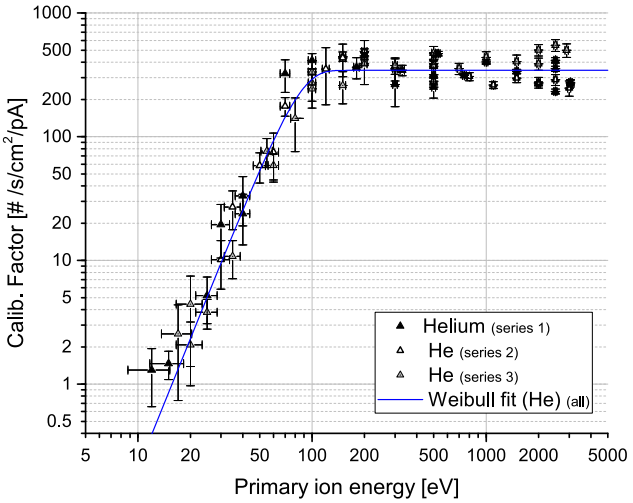

FIG. 4. Neutralizer calibration factor for helium in the energy range from 10 eV to 3 keV.

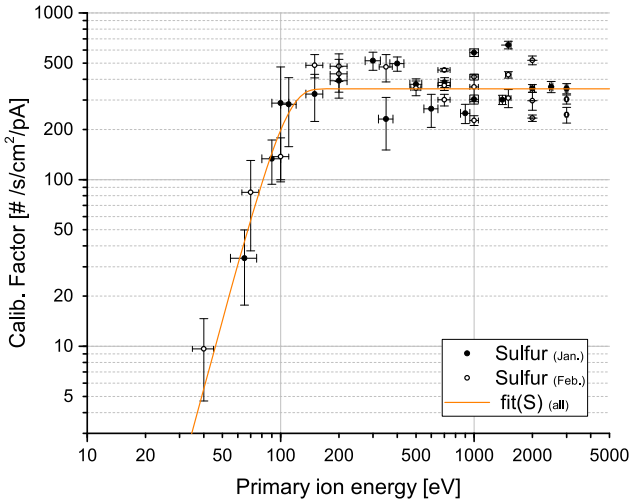

FIG. 6. Neutralizer calibration factor for sulfur in the energy range from 40 eV to 3 keV.

float potential, ion-source extraction voltage, and the plasma potential of the ion source. This difference defines the ion energy on the neutralizer surface. The relative scatter of data points is attributed to the overall system alignment accuracy, which comprises the optimized ion beam path from the source through the ion-optical system to the neutralizer and the ABM: An important step in the operation procedure of the MEFISTO calibration facility together with the neutralizer is optimizing the ion-optical beam path from the ion source to the test chamber. The optimal setting can vary slightly over time during operation. Thus, the neutralizer is positioned via a two-axis stepper motor YZ-stage to the actual ion-beam axis. Resulting in small variations in the beam incident position and direction into the neutralizer can cause some variation in its overall beam conversion efficiency, which reflects in the relative scatter of calibration factor data points.

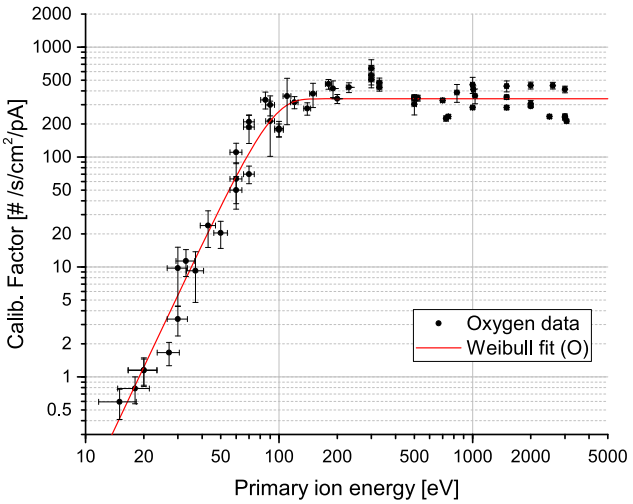

FIG. 5. Neutralizer calibration factor for oxygen in the energy range from 15 eV to 3 keV.

B. Energy loss in the neutralizer

In the ABM, time-of-flight (ToF) spectra of coincident start and stop events were recorded for ENA species H, D, He, O, and Ne at energies of the primary ion beam into the neutralizer from 3 keV down to 100 eV. From the peaks in the ToF spectra, the mean energy E_{tof} of neutral atoms scattered off the ABM start surface was

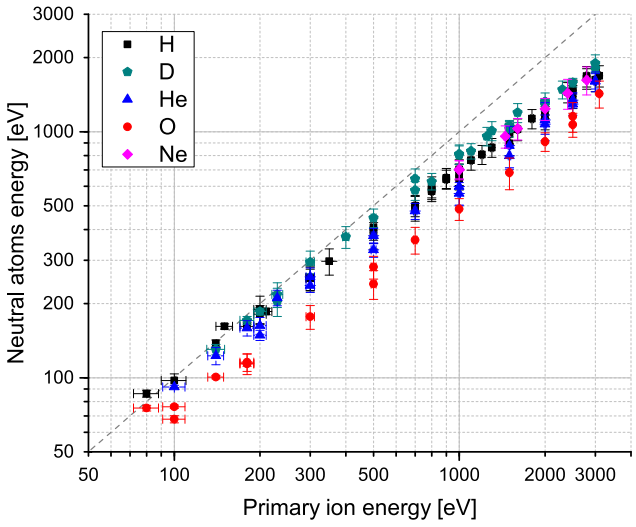

FIG. 7. ENA kinetic energy obtained from ABM ToF spectra as a function of the primary ion energy into the neutralizer for atomic species H, D, He, O, and Ne. The dashed line indicates the hypothetic case of surface scattering without energy loss.

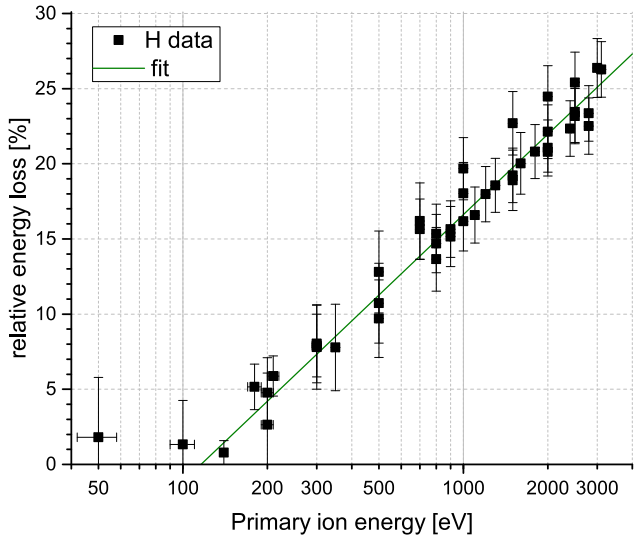

FIG. 8. Fraction of kinetic energy lost at the W surface in the neutralizer for hydrogen atoms.

retrieved by finding the center of the ToF peak by means of a Gaussian fit.[11] The results are shown in Fig. 7; the dashed line indicates the situation if no kinetic energy loss did occur on the scattering surface, i.e., $E_{tof} = E_{ion}$. The standard error of the mean of the neutral atoms' kinetic energy represents the uncertainty in determining the mean energy from the ToF spectra. The half-width at 95% of the maximum of the Gaussian fit was taken as an estimate for the standard error of the mean of the measured energy distributions. It is the accuracy with which we can determine the peak location in the energy distribution.

Figure 7 illustrates that over the full energy range, the reduction in kinetic energy tends to be more pronounced for higher atomic mass, except for the noble gas neon, for which the results are comparable to hydrogen. However, Ne spectra have just been evaluated down to 1000 eV due to a low peak signal and comparably high background in the spectra.

On their trajectory through the neutralizer and into the ABM, the atoms that generate a signal in the ToF peak were scattered at a polished W surface twice: once on the neutralizing surface in the neutralizer and once on the ABM start surface (SS). Assuming that the atoms' kinetic energy reduces by the same fraction at each surface, we obtain the relative energy loss per surface interaction as given in Eq. (10) in Ref. 11. The results are shown in Figs. 8–12, respectively, for H, D, He, O, and Ne. A log-linear two-parameter fit $[y(x) = b \cdot \ln(x) - a]$ was added to guide the eye. The fit represents the measured data reasonably well at beam energies above 100 eV (above 300 eV for deuterium).

The results presented in Figs. 8–12 show that a considerable fraction of kinetic energy is lost in the interaction with the neutralizing surface. At energies above 100 eV, the relative energy loss increases monotonically with primary ion energy from just a few percent to 20%–35% at 3 keV depending on atomic species. The fraction of energy lost tends to increase with atomic mass and is highest for oxygen among the measured atomic species.

During the instrument calibration of IBEX-Lo, the fraction of energy loss at the instrument conversion surface was determined based on the discrepancy between the instrument energy step and the set beam center energy (see Fuselier *et al.*,[4] Sec. 3.9 and Fig. 18). At energies from 100 eV to 2 keV, the fraction of energy lost was found to be[4] about 15%–30% for H and between 35% and 50% for O, with relative error bars (+0.68, −0.34). Those values were clearly higher than the 15% relative energy loss estimated before the IBEX-Lo calibration campaign but still agreed within the uncertainty range.

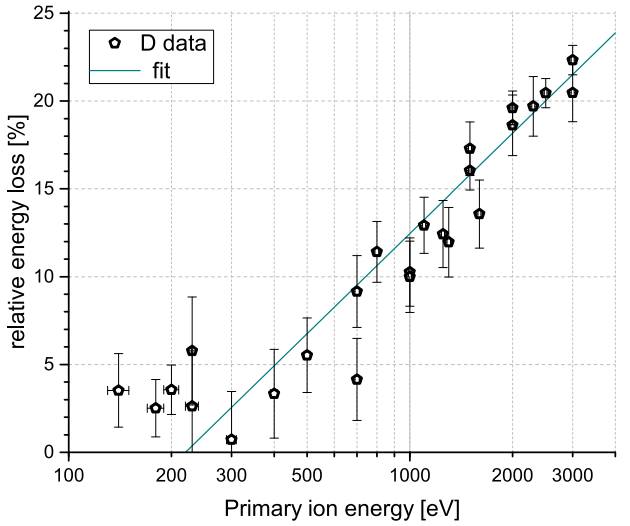

FIG. 9. Fraction of kinetic energy lost at the W surface in the neutralizer for deuterium atoms.

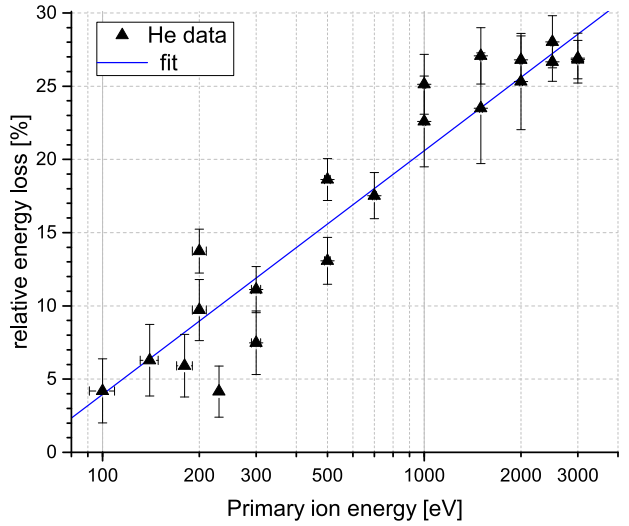

FIG. 10. Fraction of kinetic energy lost at the W surface in the neutralizer for helium atoms.

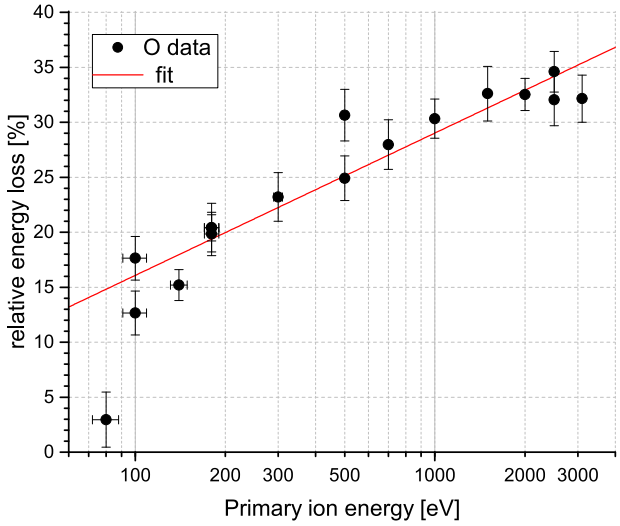

FIG. 11. Fraction of kinetic energy lost at the W surface in the neutralizer for oxygen atoms.

In comparison, the ABM measured data for hydrogen shown in Fig. 8 amount to a lower energy loss at the surface interaction, i.e., less than 10% at energies below about 400 eV but still up to 25% at the highest measured energies. For oxygen (see Fig. 11), we obtained values about 10%–20% lower than in Ref. 4. Note, however, that the IBEX-Lo CS were DLC coated Si wafers (in contrast to W single crystal in the neutralizer and in the ABM) and that the CS is installed at 15° nominal incidence angle in IBEX-Lo. Both differences could explain part of the larger energy loss derived from IBEX-Lo conversion surfaces. Overall, those results are still in agreement with the ones shown here considering the uncertainties.

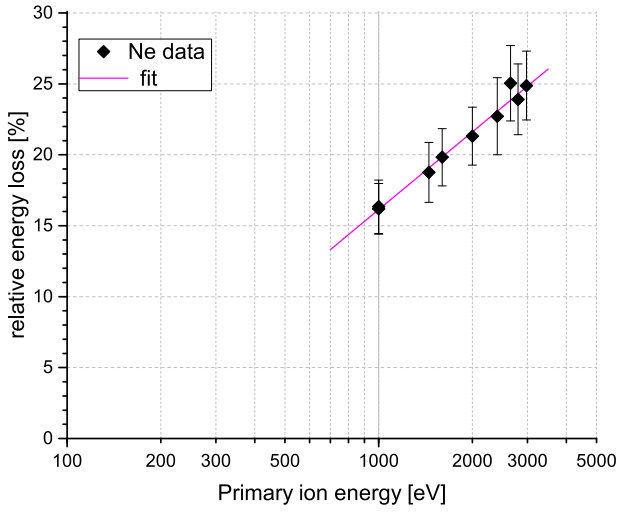

FIG. 12. Fraction of kinetic energy lost at the W surface in the neutralizer for neon atoms.

Based on the available data at low energies and the observed general trend, we expect the relative energy loss not to exceed 5% for H, D, and He at beam energies below 100 eV.

IV. SUMMARY

The low-energy neutral atom beam source in the MEFISTO laboratory[17] at the University of Bern was calibrated using the Absolute Beam Monitor[11] by relating the measured absolute neutral atom flux to the neutralizer surface current I_{ncs}.[21] With the derived calibration factors for the energy range and species of interest, the ENA flux available during calibration can be determined by real-time monitoring of the current on the neutralizer surface, I_{ncs}, and converting it to the ENA flux with the presented calibration. This work was done for the upcoming calibration campaign of the IMAP-Lo instrument. The results will also be valuable to calibrate other future ENA instruments.

Moreover, the ABM ToF spectra allowed us to determine the mean fraction of ENA kinetic energy lost at the neutralizer surface. With this knowledge, we can account for the energy loss and compensate for it by adjusting the primary ion beam accordingly.

AUTHOR DECLARATIONS

Conflict of Interest

The authors have no conflicts to disclose.

Author Contributions

Jonathan Gasser: Data curation (lead); Formal analysis (lead); Investigation (lead); Visualization (lead); Writing – original draft (lead). **André Galli**: Conceptualization (supporting); Supervision (supporting); Writing – original draft (supporting). **Peter Wurz**: Conceptualization (equal); Funding acquisition (lead); Resources (lead); Supervision (lead); Writing – original draft (supporting).

DATA AVAILABILITY

The data that support the findings of this study are available from the corresponding author upon reasonable request.

REFERENCES

[1]P. Wurz, "Detection of energetic neutral particles," *The Outer Heliosphere: Beyond the Planets* (Copernicus Gesellschaft e.V., Katlenburg-Lindau, Germany, 2000), pp. 251–288.

[2]S. A. Fuselier, A. G. Ghielmetti, T. E. Moore, M. R. Collier, J. M. Quinn, G. R. Wilson, P. Wurz, S. B. Mende, H. U. Frey, C. Jamar, J.-C. Gerard, and J. L. Burch, "Ion outflow observed by IMAGE: Implications for source regions and heating mechanisms," Geophys. Res. Lett. **28**(6), 1163–1166, https://doi.org/10.1029/2000GL012450 (2001).

[3]D. J. McComas, F. Allegrini, P. Bochsler, M. Bzowski, M. Collier, H. Fahr, H. Fichtner, P. Frisch, H. O. Funsten, S. A. Fuselier, G. Gloeckler, M. Gruntman, V. Izmodenov, P. Knappenberger, M. Lee, S. Livi, D. Mitchell, E. Möbius, T. Moore, S. Pope, D. Reisenfeld, E. Roelof, J. Scherrer, N. Schwadron, R. Tyler, M. Wieser, M. Witte, P. Wurz, and G. Zank, "IBEX—Interstellar boundary explorer," Space Sci. Rev. **146**, 11–33 (2009).

[4]S. A. Fuselier, P. Bochsler, D. Chornay, G. Clark, G. B. Crew, G. Dunn, S. Ellis, T. Friedmann, H. O. Funsten, A. G. Ghielmetti, J. Googins, M. S. Granoff,

J. W. Hamilton, J. Hanley, D. Heirtzler, E. Hertzberg, D. Isaac, B. King, U. Knauss, H. Kucharek, F. Kudirka, S. Livi, J. Lobell, S. Longworth, K. Mashburn, D. J. McComas, E. Möbius, A. S. Moore, T. E. Moore, R. J. Nemanich, J. Nolin, M. O'Neal, D. Piazza, L. Peterson, S. E. Pope, P. Rosmarynowski, L. A. Saul, J. R. Scherrer, J. A. Scheer, C. Schlemm, N. A. Schwadron, C. Tillier, S. Turco, J. Tyler, M. Vosbury, M. Wieser, P. Wurz, and S. Zaffke, "The IBEX-Lo sensor," Space Sci. Rev. **146**, 117–147 (2009).

[5]H. O. Funsten, F. Allegrini, P. Bochsler, G. Dunn, S. Ellis, D. Everett, M. J. Fagan, S. A. Fuselier, M. Granoff, M. Gruntman, A. A. Guthrie, J. Hanley, R. W. Harper, D. Heirtzler, P. Janzen, K. H. Kihara, B. King, H. Kucharek, M. P. Manzo, M. Maple, K. Mashburn, D. J. McComas, E. Moebius, J. Nolin, D. Piazza, S. Pope, D. B. Reisenfeld, B. Rodriguez, E. C. Roelof, L. Saul, S. Turco, P. Valek, S. Weidner, P. Wurz, and S. Zaffke, "The interstellar boundary explorer high energy (IBEX-Hi) neutral atom imager," Space Sci. Rev. **146**, 75–103 (2009).

[6]D. J. McComas, F. Allegrini, P. Bochsler, M. Bzowski, E. R. Christian, G. B. Crew, R. DeMajistre, H. Fahr, H. Fichtner, P. C. Frisch, H. O. Funsten, S. A. Fuselier, G. Gloeckler, M. Gruntman, J. Heerikhuisen, V. Izmodenov, P. Janzen, P. Knappenberger, S. Krimigis, H. Kucharek, M. Lee, G. Livadiotis, S. Livi, R. J. MacDowall, D. Mitchell, E. Möbius, T. Moore, N. V. Pogorelov, D. Reisenfeld, E. Roelof, L. Saul, N. A. Schwadron, P. W. Valek, R. Vanderspek, P. Wurz, and G. P. Zank, "Global observations of the interstellar interaction from the interstellar boundary explorer (IBEX)," Science **326**(5955), 959–962 (2009).

[7]N. A. Schwadron, E. Moebius, S. A. Fuselier, D. J. McComas, H. O. Funsten, P. Janzen, D. Reisenfeld, H. Kucharek, M. A. Lee, K. Fairchild, F. Allegrini, M. Dayeh, G. Livadiotis, M. Reno, M. Bzowski, J. M. Sokół, M. A. Kubiak, E. R. Christian, R. DeMajistre, P. Frisch, A. Galli, P. Wurz, and M. Gruntman, "Separation of the ribbon from globally distributed energetic neutral atom flux using the first five years of IBEX observations," Astrophys. J., Suppl. Ser. **215**(1), 13 (2014).

[8]N. A. Schwadron, F. Allegrini, M. Bzowski, E. R. Christian, M. A. Dayeh, M. I. Desai, K. Fairchild, P. C. Frisch, H. O. Funsten, S. A. Fuselier, A. Galli, P. Janzen, M. A. Kubiak, D. J. McComas, E. Moebius, D. B. Reisenfeld, J. M. Sokół, P. Swaczyna, J. R. Szalay, P. Wurz, and E. J. Zirnstein, "Time dependence of the IBEX ribbon and the globally distributed energetic neutral atom flux using the first 9 years of observations," Astrophys. J., Suppl. Ser. **239**(1), 1 (2018).

[9]A. Galli, P. Wurz, N. Schwadron, K. Fairchild, D. Heirtzler, E. Möbius, H. Kucharek, R. Winslow, M. Bzowski, M. Kubiak, I. Kowalska-Leszczynska, S. Fuselier, J. M. Sokól, P. Swaczyna, and D. McComas, "One solar cycle of heliosphere observations with the interstellar boundary Explorer: Energetic neutral hydrogen atoms observed with IBEX-Lo from 10 eV to 2 keV," Astrophys. J., Suppl. Ser. **261**(2), 18 (2022).

[10]D. J. McComas, E. R. Christian, N. A. Schwadron, N. Fox, J. Westlake, F. Allegrini, D. N. Baker, D. Biesecker, M. Bzowski, G. Clark, C. M. S. Cohen, I. Cohen, M. A. Dayeh, R. Decker, G. A. de Nolfo, M. I. Desai, R. W. Ebert, H. A. Elliott, H. Fahr, P. C. Frisch, H. O. Funsten, S. A. Fuselier, A. Galli, A. B. Galvin, J. Giacalone, M. Gkioulidou, F. Guo, M. Horanyi, P. Isenberg, P. Janzen, L. M. Kistler, K. Korreck, M. A. Kubiak, H. Kucharek, B. A. Larsen, R. A. Leske, N. Lugaz, J. Luhmann, W. Matthaeus, D. Mitchell, E. Moebius, K. Ogasawara, D. B. Reisenfeld, J. D. Richardson, C. T. Russell, J. M. Sokół, H. E. Spence, R. Skoug, Z. Sternovsky, P. Swaczyna, J. R. Szalay, M. Tokumaru, M. E. Wiedenbeck, P. Wurz, G. P. Zank, and E. J. Zirnstein, "Interstellar mapping and acceleration Probe (IMAP): A new NASA mission," Space Sci. Rev. **214**, 116 (2018).

[11]J. Gasser, A. Galli, and P. Wurz, "Absolute beam monitor: A novel laboratory device for neutral beam calibration," Rev. Sci. Instrum. **93**(9), 093302 (2022).

[12]F. Allegrini, R. W. Ebert, and H. O. Funsten, "Carbon foils for space plasma instrumentation," J. Geophys. Res.: Space Phys. **121**(5), 3931–3950, https://doi.org/10.1002/2016JA022570 (2016).

[13]J. A. Scheer, P. Wahlström, and P. Wurz, "Scattering of light molecules from thin Al_2O_3 films," Nucl. Instrum. Methods Phys. Res., Sect. B **267**, 2571–2574 (2009).

[14]P. Wahlström, J. A. Scheer, P. Wurz, E. Hertzberg, and S. A. Fuselier, "Calibration of charge state conversion surfaces for neutral particle detectors," J. Appl. Phys. **104**, 034503 (2008).

[15]P. Wurz, R. Schletti, and M. R. Aellig, "Hydrogen and oxygen negative ion production by surface ionization using diamond surfaces," Surf. Sci. **373**(1), 56–66 (1997).

[16]J. Gasser, M. Föhn, A. Galli, E. Artegiani, A. Romeo, and P. Wurz, "Cadmium telluride as a potential conversion surface," J. Appl. Phys. **129**, 045303 (2021).

[17]A. Marti, R. Schletti, P. Wurz, and P. Bochsler, "Calibration facility for solar wind plasma instrumentation," Rev. Sci. Instrum. **72**, 1354 (2001).

[18]M. Bodendorfer, P. Wurz, and M. Hohl, "Global plasma simulation of charge state distribution inside a 2.45 GHz ECR plasma with experimental verification," Plasma Sources Sci. Technol. **19**(4), 045024 (2010).

[19]M. Hohl, P. Wurz, and P. Bochsler, "Investigation of the density and temperature of electrons in a compact 2.45 GHz electron cyclotron resonance ion source plasma by X-ray measurements," Plasma Sources Sci. Technol. **14**(4), 692–699 (2005).

[20]M. Liehr, R. Trassl, M. Schlapp, and E. Salzborn, "A low power 2.45 GHz ECR ion source for multiply charged ions," Rev. Sci. Instrum. **63**(4), 2541–2543 (1992).

[21]M. Wieser and P. Wurz, "Production of a 10 eV–1000 eV neutral particle beam using surface neutralization," Meas. Sci. Technol. **16**, 2511–2516 (2005).